JOURNAL OF GUIDANCE, CONTROL, AND DYNAMICS
Vol. 33, No. 6, November–December 2010

Engineering Notes

Optimal Guidance of Low-Thrust Trajectories

Jesus Gil-Fernandez*
GMV, 28760 Madrid, Spain
and
Miguel A. Gomez-Tierno†
Technical University of Madrid, 28040 Madrid, Spain

DOI: 10.2514/1.51043

Nomenclature

$\mathbf{F_K}$	=	input-influence matrix at t_K
$\mathbf{g_K}$	=	gravitational acceleration at t_K
I	=	identity matrix
I_{SP}	=	specific impulse
m_K	=	mass at t_k
$\mathbf{r}_K$	=	position at t_k
$\mathbf{T_K}$	=	thrust at t_k
t	=	time
$\mathbf{u_K}$	=	control at t_K
ν, η	=	Lagrange multipliers
$\mathbf{x}$	=	state vector
$\delta\mathbf{u_K}$	=	correction to nominal control at t_K
μ	=	gravity parameter
$: \prod_{\mathbf{K}=\mathbf{i}}^{\mathbf{N}-\mathbf{1}} \varphi_{\mathbf{K}+\mathbf{1},\mathbf{K}} :$	=	time-ordered product
$\varphi_{\mathbf{K}+\mathbf{1},\mathbf{K}}$	=	transition matrix from t_K to t_{K+1}

I. Introduction

ELECTRIC propulsion has been selected in several interplanetary missions due to its higher efficiency compared with chemical propulsion. Perturbations such as maneuver execution errors, navigation uncertainties, operational constraints, uncertain parameters (e.g. initial state), and disturbance forces, produce deviations from the reference trajectory that the guidance and control functions must cancel at the expense of additional propellant mass.

NASA Deep Space 1 mission proved an autonomous low-thrust guidance method [1] based on linearization of the terminal state in terms of a certain parameterization of the thrust profile. The terminal controller [2] was solved via Lagrange multipliers. This method has been refined [3] including a line search during the improvement step in order to assure convergence in case of poorly defined reference trajectory (e.g. sparse nodes, low numerical resolution).

An interesting finite-thrust guidance and control method has been applied to small-body proximity operations [4]. It is based on pseudowaypoints generation and linear matrix inequality based feedback control. Waypoint-based, autonomous guidance with low-thrust propulsion was implemented for the approach phase of rendezvous missions to small asteroids [5]. The thrust profile was parameterized using a simple law that reduces the guidance problem to solve a system of nonlinear equations. Another autonomous guidance algorithm [6] used the Pontryagin minimum principle [2] to derive the optimal corrections to the nominal thrust profile minimizing the propellant consumption. Receding horizon control has been analyzed [7] using direct transcription to discretize the optimal control problem and an interior-point algorithm to solve numerically the resulting nonlinear programming problem.

The optimal guidance and control methods presented in this paper focus on closed-form algorithms as in Deep Space 1 autonomous guidance [1], with special emphasis on the propagation and computation of the required partial derivatives matrices. The guidance function is a terminal controller that aims to reach the next waypoint at a specific time. A receding horizon control maintains the spacecraft in the proximity of the reference trajectory during the thrusting arc. The main differences with the aforementioned methods are that the optimal guidance and control laws are derived on a closed-form solution and accommodate thrust constraints in magnitude and direction. These qualities make them suitable for operational use even in autonomous guidance, navigation and control systems [8].

II. Problem Formulation

The main hypothesis is that the deviations from the reference trajectory are small and can be corrected with small variations in the reference thrust profile. The presented guidance and control methods are based on a certain discretization of the trajectory and thrust [4]. The trajectory is divided in N segments of equal duration, except the last one that completes the required transfer time. In each segment, the gravity field is approximated by a linear expansion at the initial node. Considering a zero-order hold approach for the control acceleration, the resulting dynamics is a piecewise linear time-invariant (LTI) system. The equations of motion at a segment K are presented in Eq. (1). The initial value for the state $\mathbf{x_K}$ and thrust $\mathbf{T_K}$ are taken from the reference trajectory:

$$\dot{\mathbf{x}}_\mathbf{K} = \underbrace{\begin{bmatrix} \mathbf{0} & \mathbf{I} \\ \mathbf{G_K} & \mathbf{0} \end{bmatrix}}_{\mathbf{A_K}} \cdot \mathbf{x_K} + \underbrace{\begin{bmatrix} \mathbf{0} \\ \mathbf{I} \end{bmatrix}}_{B} \cdot (\tilde{\mathbf{g}}_\mathbf{K} + \mathbf{u_K})$$

$$\mathbf{G_K} = \nabla \mathbf{g}|_{\mathbf{r_K}} = \frac{\mu}{r_K^3}\left(\frac{3}{r_K^2}\mathbf{r_K} \cdot \mathbf{r_K^T} - \mathbf{I}\right)$$

$$\tilde{\mathbf{g}}_\mathbf{K} = \mathbf{g_K} - \mathbf{G_K}\mathbf{r_K}$$

$$\mathbf{u_K} = \mathbf{T_K}/m_K$$

$$\dot{m}_K = -\frac{\|\mathbf{u_K}\|}{I_{SP}g_0} m_K \tag{1}$$

The guidance function must compute an acceleration profile correction that takes the spacecraft to the desired state at a given time, and produces a trajectory as close as possible to the reference trajectory. The guidance problem is mathematically formulated as a finite-horizon optimal control problem presented in Eq. (2). The cost function is the sum of squares of the control corrections, in order to minimize the deviations from the optimal thrust profile. A quadratic objective function is typical in guidance and control methods [1,2]. The control variables are accelerations provided by the thrusters in each segment. Only the thrusting segments in the reference trajectory are included in the control vector. The thrusting time is kept constant, contrary to other strategies that varies the thrust duration [1,3]. To assure controllability, the reference thrust profile must include a margin with respect to the maximum thrust, so that the thrust magnitude can be increased as result of the control corrections computed by the guidance.

Received 4 June 2010; revision received 12 July 2010; accepted for publication 12 July 2010.

*Technical Consultant, Advanced Space Systems and Technologies, Isaac Newton 11, Tres Cantos. Senior Member AIAA.

†Director of the School of Aerospace Engineering and Full Professor of Flight Mechanics, Plaza Cisneros 3. Member AIAA.

The path constraints are the dynamics [Eq. (1)], and the maximum available thrust. The maximum control acceleration changes from segment to segment due to the propellant mass expenditure. The acceleration constraint in Eq. (2) considers a single engine providing the entire thrust, which is the typical case for interplanetary probes. In [8], this constraint is formulated for multiple thrusters because the weak dynamics near small bodies allows using the attitude management thrusters for trajectory guidance and control:

$$\min_{\delta\{\mathbf{u_K}\}} J = \frac{1}{2}\sum_{K=0}^{N-1} \|\delta\mathbf{u_K}\|^2, \quad \text{subject to}$$
$$\begin{cases} \dot{\mathbf{x}}_\mathbf{K} = \mathbf{A_K}\mathbf{x_K} + \mathbf{B}(\tilde{\mathbf{g}}_\mathbf{K} + \mathbf{u_K} + \delta\mathbf{u_K}), & \forall\ k = 0,\ldots,N-1 \\ \mathbf{x_N} = \mathbf{x_f} & \\ \|\mathbf{u_K} + \delta\mathbf{u_K}\| \le a_{K\max}, & \forall\ k = 0,\ldots,N-1, \quad \text{where } a_{K\max} = T_{\max}/m_K,\ m_K = m_{K-1}e^{-\|\mathbf{u}_{\mathbf{K}-1}+\delta\mathbf{u}_{\mathbf{K}-1}\|(t_K-t_{K-1})/I_{\mathrm{SP}}g_0} \end{cases} \tag{2}$$

The LTI system defined in Eq. (1) can be solved analytically providing an explicit formulation for the transition and input-influence matrices [Eq. (3)]. Hence, the final state is known as a linear function of the initial state and the control vector [Eq. (4)]. This analytical propagation is very helpful for guidance and control purposes since it provides the analytical partial derivatives in the same propagation call with no need of additional computations, i.e., no integration of the variational equations or numerical differentiation:

$$\begin{aligned} &\mathbf{x_{K+1}} = \boldsymbol{\varphi}_{\mathbf{K+1,K}} \cdot \mathbf{x_K} + \mathbf{F_K} \cdot (\tilde{\mathbf{g}}_\mathbf{K} + \mathbf{u_K}) \\ &\boldsymbol{\varphi}_{\mathbf{K+1,K}} = e^{\mathbf{A_K}(t_{K+1}-t_K)} \\ &\mathbf{F_K} = \int_{t_K}^{t_{K+1}} e^{\mathbf{A_K}(t_{K+1}-\tau)}\mathbf{B}\,\mathrm{d}\tau \end{aligned} \tag{3}$$

$$\mathbf{x_N} = \boldsymbol{\Phi}_{\mathbf{N,0}} \cdot \mathbf{x_0} + \underbrace{[\,\boldsymbol{\Phi}_{\mathbf{N,1}}\mathbf{F_0} \quad \boldsymbol{\Phi}_{\mathbf{N,2}}\mathbf{F_1} \quad \ldots \quad \mathbf{F_{N-1}}\,]}_{\boldsymbol{\Psi}_{\mathbf{N,0}}} \cdot \underbrace{\begin{Bmatrix} \tilde{\mathbf{g}}_\mathbf{0} + \mathbf{u_0} \\ \vdots \\ \tilde{\mathbf{g}}_\mathbf{N-1} + \mathbf{u_{N-1}} \end{Bmatrix}}_{\{\tilde{\mathbf{g}}_\mathbf{K} + \mathbf{u_K}\}_{\mathbf{0,N-1}}}$$
$$\boldsymbol{\Phi}_{\mathbf{N,i}} =: \boldsymbol{\Pi}_{\mathbf{K=i}}^{\mathbf{N-1}} \boldsymbol{\varphi}_{\mathbf{K+1,K}} : \tag{4}$$

The accuracy of the analytical propagation scheme is analyzed in detail since propagation errors will cause additional propellant expenditure. The results are compared with a fourth-order Runge–Kutta numerical integration scheme. This numerical scheme is implemented to compute the reference optimal trajectories for the test scenarios [9]. The first Earth–Earth transfer of the BepiColombo mission [10], depicted in Fig. 1, is taken as testbench. The position difference between the numerical and analytical integration schemes is presented in Fig. 2. The error of the analytical propagation scheme is acceptable for the scenarios subject of analysis. Thrust arcs produce few tens kilometers of error at the waypoints (end of thrust arc), which is 1 order of magnitude smaller than the uncertainties and perturbations considered in the simulations.

By means of the analytical propagation [Eq. (4)], the finite-horizon optimal control problem of Eq. (2) is transformed into a constrained parameter optimization problem [2]. The resulting guidance problem is given in Eq. (5):

$$\min_{\delta\{\mathbf{u_K}\}} J = \frac{1}{2}\sum_{K=0}^{N-1} \|\delta\mathbf{u_K}\|^2, \quad \text{subject to}$$
$$\begin{cases} \boldsymbol{\Phi}_{\mathbf{N,0}}\mathbf{x_0} + \boldsymbol{\Psi}_{\mathbf{N,0}}\{\tilde{\mathbf{g}}_\mathbf{K} + \mathbf{u_K} + \boldsymbol{\delta}\mathbf{u_K}\}_{\mathbf{0,N-1}} = \mathbf{x_f} & \\ \|\mathbf{u_K} + \boldsymbol{\delta}\mathbf{u_K}\| \le a_{K\max}, & \forall\ k = 0,\ldots,N-1, \ \text{where } a_{K\max} = T_{\max}/m_K,\ m_K = m_{K-1}e^{-\|\mathbf{u}_{\mathbf{K}-1}+\delta\mathbf{u}_{\mathbf{K}-1}\|(t_K-t_{K-1})/I_{\mathrm{SP}}g_0} \end{cases} \tag{5}$$

III. Optimal Guidance Schemes

Two guidance algorithms are presented to solve the constrained parameter optimization defined in Eq. (5). The main difference between them is the technique to deal with the thrust constraint. The first method solves the guidance problem in two steps. The first step consists on finding the unconstrained control correction that achieves the desired final state. In the second step, the thrust constraint fulfillment is forced in each segment. The unconstrained problem can be solved adjoining the final state constraint to the cost function via Lagrange multipliers [Eq. (6)]:

$$\min_{\delta\{\mathbf{u_K}\}} J = \frac{1}{2}\sum_{K=0}^{N-1} \|\delta\mathbf{u_K}\|^2 + \boldsymbol{\nu}\cdot(\mathbf{x_f} - \mathbf{x_N} - \boldsymbol{\Psi}_{\mathbf{N,0}}\{\delta\mathbf{u_K}\}_{0,N-1})$$
$$\mathbf{x_N} = \boldsymbol{\Phi}_{\mathbf{N,0}}\mathbf{x_0} + \boldsymbol{\Psi}_{\mathbf{N,0}}\{\tilde{\mathbf{g}}_\mathbf{K} + \mathbf{u_K}\}_{\mathbf{0,N-1}} \tag{6}$$

The control correction vector that solves Eq. (6) is obtained explicitly with the Gauss pseudoinverse of the input-influence matrix [1], and is presented in Eq. (7). In the second step, the control vector of the segments with active constraints is projected onto the boundary. Then, the final state is evaluated with the new thrust profile. If the required final state is not achieved, the guidance scheme starts again considering only the control segments with nonactive constraints:

$$\delta\{\mathbf{u_K}\} = \boldsymbol{\Psi}_{\mathbf{N,0}}^{\mathbf{T}}(\boldsymbol{\Psi}_{\mathbf{N,0}}\boldsymbol{\Psi}_{\mathbf{N,0}}^{\mathbf{T}})^{-1}\boldsymbol{\Delta}\mathbf{x_N} \qquad \boldsymbol{\Delta}\mathbf{x_N} = \mathbf{x_f} - \mathbf{x_N} \tag{7}$$

In the second guidance method, the thrust constraint is included in the calculation of the control correction vector. The segments with active constraints form a subset A and are not removed from the control vector. The first order expansion of the thrust constraint [Eq. (8)] is also adjoined to the cost function [Eq. (9)]. Thus, the segments with active thrust constraint are included in the control vector but the thrust correction vector is forced to be on the plane tangent to the sphere with radius T_{MAX}. Therefore, each segment with active thrust constraint contributes only 2 degrees of freedom to the control vector:

$$(\mathbf{u_A} + \boldsymbol{\delta}\mathbf{u_A})\cdot(\mathbf{u_A} + \boldsymbol{\delta}\mathbf{u_A}) = 1,$$
$$\forall\ A/\{\|\mathbf{u_A}\| = T_{\mathrm{MAX}}/m_A\} \overset{\delta\mathbf{u_A}\ll\mathbf{u_A}}{\longrightarrow} \mathbf{u_A}\cdot\delta\mathbf{u_A} = 0 \tag{8}$$

$$\min_{\delta\{\mathbf{u_K}\}} J = \frac{1}{2}\sum_{K=0}^{N-1} \|\delta\mathbf{u_K}\|^2 + \boldsymbol{\nu}\cdot(\boldsymbol{\Delta}\mathbf{x_N} - \boldsymbol{\Psi}_{\mathbf{N,0}}\{\delta\mathbf{u_K}\}_{\mathbf{0,N-1}}) + \boldsymbol{\eta}\cdot(\mathbf{U_A}\cdot\{\delta\mathbf{u_A}\})$$
$$\mathbf{U_A} = \begin{bmatrix} \mathbf{u}_{\mathbf{A_1}}^{\mathbf{T}} & & \mathbf{0} \\ & \ddots & \\ \mathbf{0} & & \mathbf{u}_{\mathbf{A_m}}^{\mathbf{T}} \end{bmatrix} \tag{9}$$

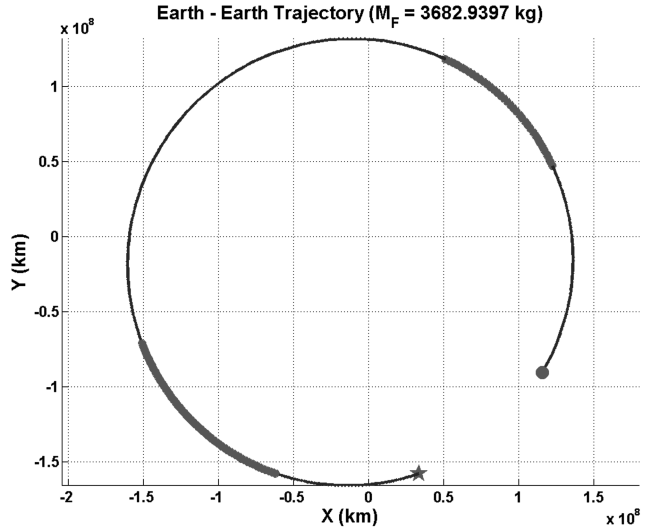

Fig. 1 Trajectory in ecliptic plane; bold line indicates thrust arcs.

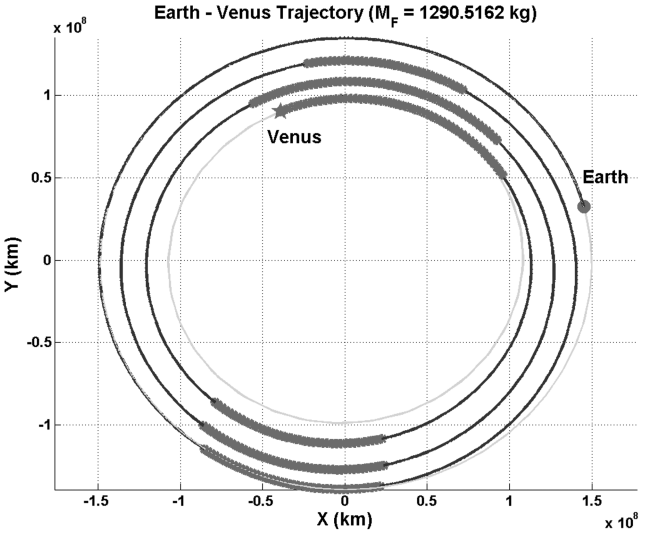

Fig. 3 Optimal Earth–Venus transfer.

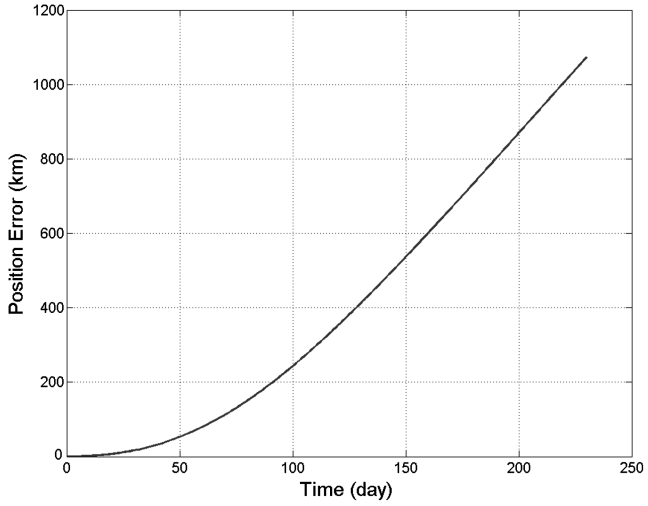

Fig. 2 Position difference between the propagation schemes.

The optimal Newton step that solves the constrained parameter optimization problem of Eq. (9) is given in Eq. (10). The control correction vector of the active segments must be much smaller than the reference control for the Eq. (8) to be valid. All the segments with active constraint are projected onto the boundary and included in the subset A for the next iteration. Then, the final state is computed with the new control vector. If the residual is larger than a given tolerance, the guidance scheme starts again:

$$\delta\{\mathbf{u_K}\} = \mathbf{\Psi}_{\mathbf{N},\mathbf{0}}^{\mathbf{T}}(\mathbf{\Psi}_{\mathbf{N},\mathbf{0}}\mathbf{\Psi}_{\mathbf{N},\mathbf{0}}^{\mathbf{T}})^{-\mathbf{1}}\Delta\mathbf{x_N} - \mathbf{M_A}\mathbf{U_A^T}(\mathbf{U_A}\mathbf{M_A}\mathbf{U_A^T})^{-\mathbf{1}}\mathbf{U_A}(\mathbf{\Psi}_{\mathbf{N},\mathbf{0}}^{\mathbf{T}}(\mathbf{\Psi}_{\mathbf{N},\mathbf{0}}\mathbf{\Psi}_{\mathbf{N},\mathbf{0}}^{\mathbf{T}})^{-\mathbf{1}})_{\mathbf{A}}\Delta\mathbf{x_N} \quad (10)$$

$$\mathbf{M_A} = (\mathbf{\Psi}_{\mathbf{N},\mathbf{0}}^{\mathbf{T}}(\mathbf{\Psi}_{\mathbf{N},\mathbf{0}}\mathbf{\Psi}_{\mathbf{N},\mathbf{0}}^{\mathbf{T}})^{-\mathbf{1}}\mathbf{\Psi}_{\mathbf{N},\mathbf{0}})_{\mathbf{A}} - \mathbf{I}$$

IV. Validation

An optimal Earth–Venus transfer from [9] is taken as testbench (Fig. 3). For guidance purposes, the transfer is reoptimized considering 95% of the maximum available thrust. The guidance objective is the Venus position and velocity at the end of the transfer. The control segments are all the thrusting segments of the reference trajectory. The discretization of the dynamics produces a deviation in the final state. In this validation case, due to the long transfer and the multiple thrust arcs, the deviation of the propagation at the end of the transfer can be million kilometers. The most significant contribution comes from the zero-order-hold approach.

A Monte Carlo simulation (200 cases) is executed varying the initial state from the reference trajectory. The initial position and velocity have a large dispersion from a uniform distribution ($[-100.000,\ 100.000]$ km, and $[-10,\ 10]$ m/s). Because of the far guidance horizon (2.73 years), small deviations in the initial state propagate to very large final deviations. In this scenario, the two-step method is more efficient in terms of mass expenditure (Fig. 4) than the single-step method. The guidance mass distributions are centered on the value required to compensate the impact of the discretization. Regarding the computational time, the single-step algorithm is faster than the one step-algorithm, in most cases (90% percentile is 5.5 s in the single-step method and 7 s in the two-step method). However, the maximum computational time in the single-step guidance (10 s) is longer than in the two-step algorithm (shorter than 8 s). The computational times are taken in a laptop with an Intel Core 2 Duo processor at 2.40 GHz.

For the two-step method, which is the most promising for practical applications, the initial dispersion is increased until at least one Monte Carlo realization does not converge. The initial position dispersion at which the two-step method fails is 500,000 km (1σ), and the initial velocity is 70 m/s (1σ). These limits are increased optimizing the reference trajectory with a higher margin in the maximum thrust. There are different possibilities if nonconvergence arises such as reoptimize the entire trajectory or adding thrust segments at the end of the thrust arc [1,3].

V. Application to BepiColombo

An implementation of the guidance algorithms is applied to the first arc of the BepiColombo mission [10]. This mission aims at Mercury using solar electric propulsion after numerous gravity assists with Earth, Venus, and Mercury. The maximum available thrust depends on the heliocentric distance. The thrust solar aspect angle (SAA) is constrained within some limits that also vary with the heliocentric distance. There must be coast arcs of few weeks after departure and before arrival. The first arc is an Earth–Earth transfer including two thrust arcs. The trajectory is reoptimized [9] reducing the maximum thrust level by 10% and the SAA constraints by 3° (Fig. 1).

The guidance function is executed at the beginning of a thrust arc and its objective is the state of the reference trajectory at the end of the thrusting arc. Additionally, a control function implements the same algorithm as a receding horizon control executed after each segment. The constraints on the thrust level and SAA must be fulfilled by the

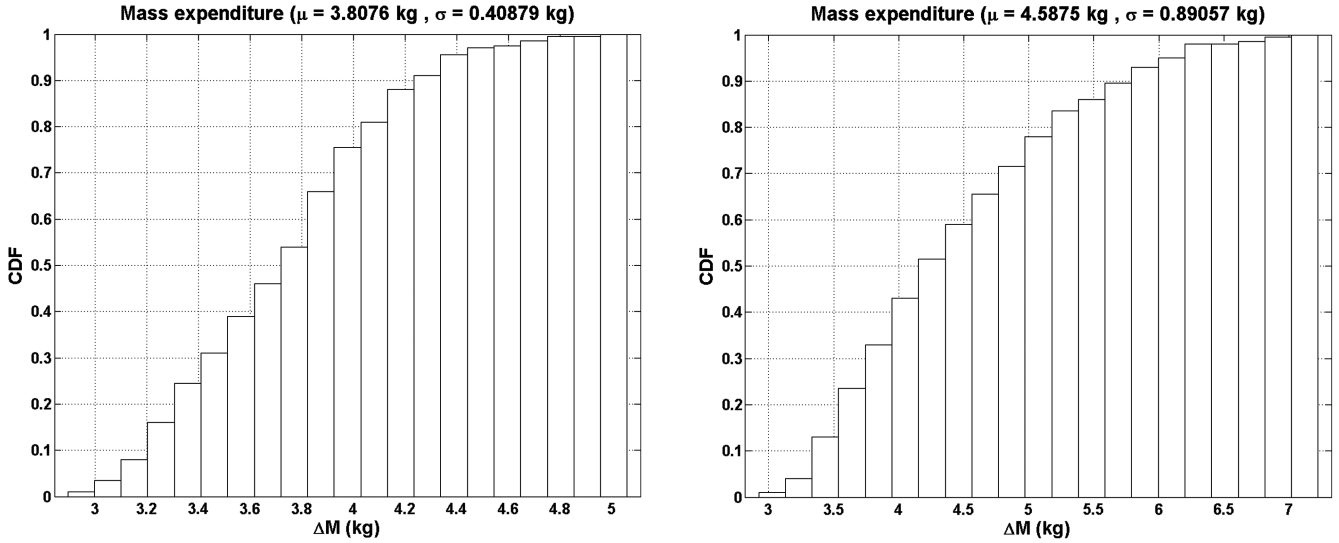

a) Two-step method **b) Single-step method**

Fig. 4 CDF of the propellant expenditure.

profile resulting after the guidance and control corrections. The formulation of the optimal control problem including the thrust SAA constraint is given in Eq. (11). The two-step method is selected as the guidance and control algorithm because produces lower mass expenditure and smaller number of active segments, and the inclusion of the constraint on the thrust direction is straightforward. All the constraints on the thrust are imposed at the same time during the second step. The boundaries are defined by the thrust magnitude and direction:

$$\min_{\delta\{\mathbf{u_K}\}} J = \frac{1}{2}\sum_{K=0}^{N-1} \|\delta\mathbf{u_K}\|^2, \quad \text{subject to}$$

$$\mathbf{\Phi_{N,0}x_0} + \mathbf{\Psi_{N,0}}\{\tilde{\mathbf{g}}_\mathbf{K} + \mathbf{u_K} + \boldsymbol{\delta}\mathbf{u_K}\}_{\mathbf{0,N-1}} = \mathbf{x_f}$$

$$\|\mathbf{u_K} + \boldsymbol{\delta}\mathbf{u_K}\| \le a_{K\max}, \quad \forall\ k = 0, \ldots, N-1$$

$$\cos SAA_{\max} \le \frac{\mathbf{u_K} + \boldsymbol{\delta}\mathbf{u_K}}{\|\mathbf{u_K} + \boldsymbol{\delta}\mathbf{u_K}\|} \cdot \frac{\mathbf{r_K}}{r_K} \le \cos SAA_{\min}$$

$$\forall\ k = 0, \ldots, N-1 \tag{11}$$

A Monte Carlo simulation is executed to test the performances of the guidance and control algorithms. Each component of the initial state is dispersed independently with a uniform distribution ($[-30000, \ 30000]$ km, $[-3, \ 3]$ m/s). These initial deviations are deemed conservative and translate into deviations of 1e6 km at the end of the arc (Fig. 5). The cumulative distribution function (CDF) of the mass expenditure corresponding to the guidance alone is presented in Fig. 6. The maximum computational time required by the guidance is less than 4.5 s. The maximum number of active segments is 35, the average is 4, and the 90% percentile is 13.

The navigation uncertainty is modeled as an exponentially correlated colored noise [11]. Each component of the estimated state has an independent error with standard deviation of 300 km (position) or 0.1 m/s (velocity), and time constant five days. The estimated state is updated after each segment (one day). The navigation errors for a Monte Carlo realization are presented in Fig. 7. In addition, thrust execution errors are also included considering standard deviation of 1% in magnitude and 1° in direction.

The deviations produced by these errors and uncertainties are corrected by the receding horizon control. The control parameters are traded to maintain the position deviation within bounds similar to the considered navigation error (note that an initial velocity error of 1 m/s will produce a position deviation of few 100 km after few days). The CDF of the total mass expenditure including guidance and

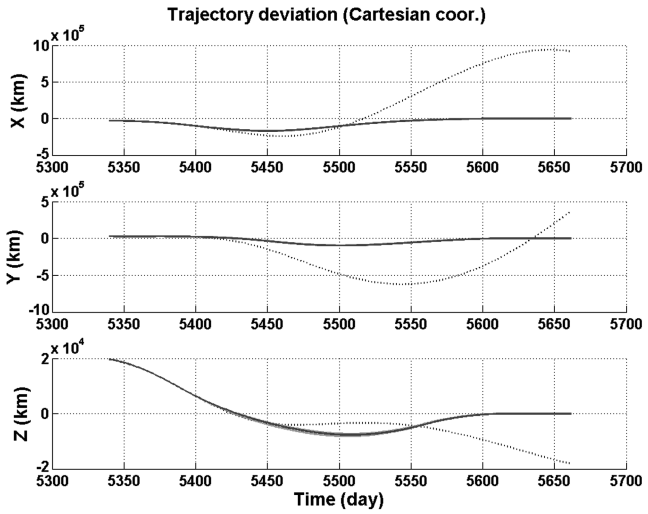

Fig. 5 Trajectory deviation (dotted line: no guidance; solid line: guidance).

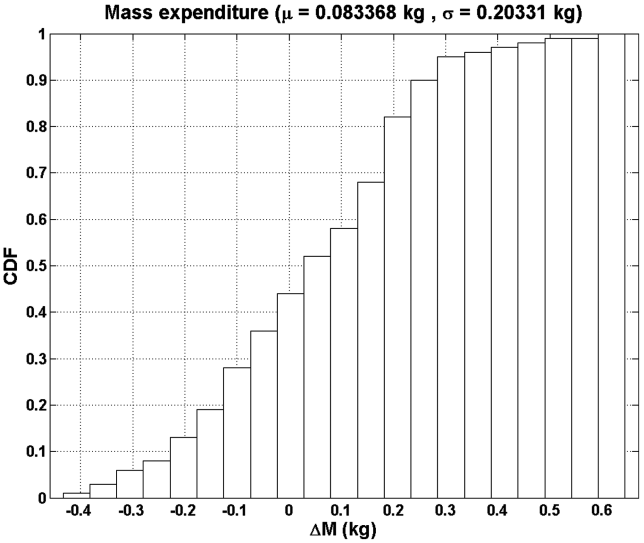

Fig. 6 Guidance performances.

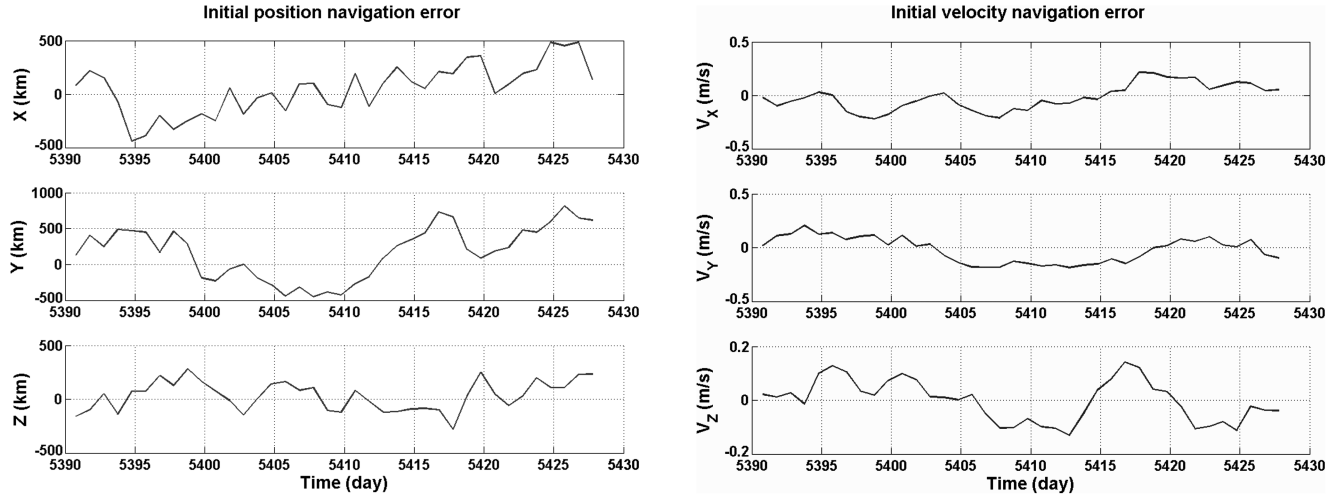

Fig. 7 Position and velocity navigation errors.

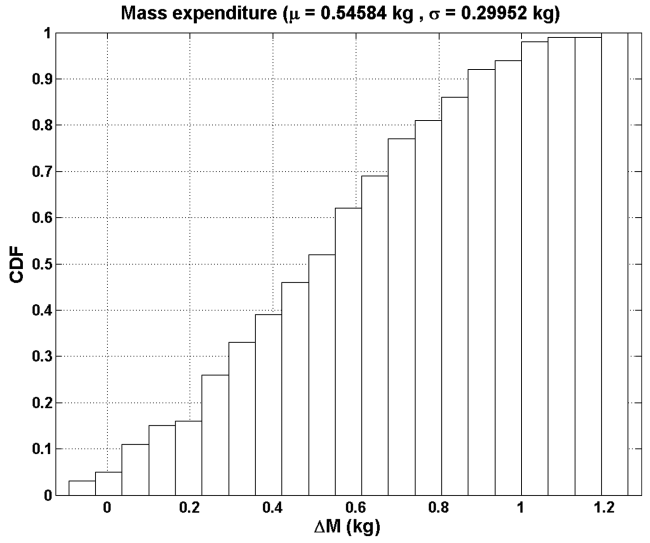

Fig. 8 Guidance and control performances.

control is presented in Fig. 8. The average computational time of the control function is 0.025 s and the maximum is less than 0.037 s.

VI. Conclusions

Optimal guidance methods for flying interplanetary low-thrust trajectories have been described. An analytical propagation scheme provides the guidance derivatives in closed form. The finite-horizon optimal control problem is transformed into a constrained parameter optimization and two methods have been presented to solve it. Both guidance methods have been benchmarked in a complex scenario, showing good performances and short computation time. Monte Carlo analysis on a BepiColombo arc with operational constraints shows the good preliminary performances of the two-step guidance and control algorithm. Practical applications are autonomous guidance, navigation and control systems, and propellant budget estimation for mission analysis.

Acknowledgments

We are grateful to Tomas Prieto-Llanos at GMV for his wise advice on astronautics, and to Mariella Graziano at GMV for her support to mission analysis research.

References

[1] Riedel, J. E., Bhaskaran, S., Desai, S., Han, D., Kennedy, B., Null, G. W. et al., "Autonomous Optical Navigation (AutoNav) DS1 Technology Validation Report," Jet Propulsion Lab. (California Inst. of Technology) Rept. 00-10,26 April 2004.

[2] Bryson, A. E., and Ho, Y. C., *Applied Optimal Control: Optimization, Estimation, and Control*, 2nd ed., Hemisphere, Washington, D.C., 1975, Chap. 5.

[3] Gil-Fernández, J., Graziano, M., Milic, E., and Gómez Tierno, M. A., "Guidance Scheme for Autonomous Electric Propelled Spacecraft," *Space Technology*, Vol. 24, Nos. 2–3, 2004, pp. 157–167.

[4] Carson, J. M., and Acikmese, A. B., "Small Body GN and C Research Report: A Guidance and Control Technique for Small-Body Proximity Operations with Guaranteed Guidance Resolvability and Required Thruster Silent Time," Jet Propulsion Lab. (California Inst. of Technology) Document D-32948, Sept. 2005.

[5] Gil-Fernández, J., Cadenas-Gorgojo, R., Prieto-Llanos, T., Graziano, M., and Drai, R., "Autonomous GNC Algorithms for Rendezvous Missions to Near-Earth-Objects," AIAA/AAS Astrodynamics Specialist Conference and Exhibit, AIAA Paper 2008-7087, Honolulu, HI, 18–21 Aug. 2008

[6] Gipsman, A., Guelman, M., and Kogan, A., "Autonomous Navigation and Guidance System for Low Thrust Driven Deep Space Missions," *Acta Astronautica*, Vol. 44, Nos. 7–12, 1999, pp. 353–364. doi:10.1016/S0094-5765(99)00058-2

[7] Arrieta-Camacho, J. J., and Biegler, L. T., "Real Time Optimal Guidance of Low-Thrust Spacecraft: An Application of Nonlinear Model Predictive Control," *Annals of the New York Academy of Sciences*, Vol. 1065, 2005, pp. 174–188.

[8] Gil-Fernandez, J., and Graziano, M., "Autonomous GNC for Descent and Landing on Small, Irregular Bodies," 20th AAS/AAIA Space Flight Mechanics Meeting, AAS Paper 10-256, San Diego, CA, Feb. 14–17.

[9] Gil-Fernandez, J., and Gomez-Tierno, M. A., "Practical Method for Optimization of Low-Thrust Transfers," *Journal of Guidance, Control, and Dynamics*, Vol. 33, No. 6, 2010, pp. 1927–1931. doi:10.2514/1.50739

[10] Garcia, D., Jehn, R., Schoenmaekers, J., and de Pascale, P., "BepiColombo Mercury Cornerstone Consolidated Report on Mission Analysis," ESA/European Space Operations Center, Mission Analysis Office Working Paper No. 525, 01 April 2010.

[11] Bierman, G. J., *Factorization Methods for Discrete Sequential Estimation*, Academic Press, New York, 1977, pp. 150–152.